AN ACCURATE PARTIAL SHADING DETECTION AND GLOBAL MAXIMUM POWER POINT TRACKING TECHNIQUE BASED ON IMAGE PROCESSING

Ahmed K Ryad[*] – Ahmed M Atallah – Abdelhalim Zekry

Faculty of Engineering, Ain Shams University, Cairo, Egypt

ARTICLE INFO

***Article history*:**
Received: 26.4.2020.
Received in revised form: 8.9.2020.
Accepted: 11.9.2020.

Keywords:
Global Maximum Power Point Tracking
Partial Shading,
Partial Shading Detection,
Artificial Vision
Camera Response Function

DOI: https://doi.org/10.30765/er.1636

Abstract:

This paper aims to detect the existence of partial shading conditions on the PV array and to estimate the vicinity of the global maximum power point for shaded PV modules based solely on the captured image of the PV modules. Detecting the existence of partial shading is based on comparing the average image pixel intensity for each PV module to find any mismatch in the incident irradiance. Estimating the incident irradiance level of each PV module is based on the camera response function with the help of a reference module. Furthermore, after estimating the irradiance intensity on the modules, we used the captured image for each PV module to detect the shaded area percentage. Detect the presence of partial shading conditions and estimating the position of the Global Maximum Power Point under partial shading was achieved with simple and cheap procedure yet effective at various shading patterns regardless of the environmental circumstances.

1 Introduction

Partial shading (PS) is the phenomenon of un-equal irradiance dispersion over PV modules, leading to the hotspots occurrence and much power losses as shaded modules consume power due to reverse bias [1]. Bypass diodes are used to prevent reverse biasing for shaded modules providing an alternative path through diodes to the series-connected modules, thus preventing hotspot formation and modules aging. However, adding bypass diodes significantly changes the photovoltaic (PV) module P-V single-peak curve to a multi-peak curve with several local peaks depending on the shading pattern shape and intensity. The existence of only one global peak makes the maximum power point tracking (MPPT) system more complicated [2].
Various research aims to mitigate the PS effect with different approaches.

One of the most popular approaches is the optimization techniques aiming to find the GMPP and evade the local minima points, although this approach suffers various limitations as dependability on the initial condition and tuning parameters, excess iterations, complex hardware implementation [3].
Another approach is the model-based approach utilizing the PV array equations to estimate the region(s) of the GMPP, although this approach suffers from excessive mathematical computation and depends on various voltage and current measurements [4].

To avoid excessive computation another approach in [5] suggests direct computation for the position of the GMPP without the need for excessive computations, although the method accuracy relies heavily on key parameters that need to be estimated first, and need various measurements to estimate irradiance level. Reconfiguration approaches tend to increase the array output at partial shading conditions via altering the electric switches connection the PV array, this approach improves the array performance at partial shading circumstances, although the need for a switching matrix and excessive computations are major concerns to this approach [6], [7].

System compensation is another approach to increase the system output at partial shading through restoring the system normal condition at uniform irradiance with the aid of power electronics circuitry mainly

[*] *Corresponding author*
E-mail address: eng_ahmed_ryad@yahoo.com

converters. This approach brings the system again to single peak behavior making the MPPT process easier, but on the expenses of the increasing system cost, more complicated design, extra power electronics needed at harsh environmental conditions [8].

Another approach makes use of artificial vision techniques. In [9], images from the webcam are used to detect the shading region then estimate shading irradiance and shading ratio to provide a reference voltage corresponding to the GMPP. Although this technique is mainly dependent on the accuracy of the estimation process and doesn't detect shading conditions. While in [10] images captured from the webcam are used to measure rather than estimate irradiance incidence on PV array then a global maximum power estimator technique is used to track GMPP, the method is easy and cheap but again heavily dependent on the accuracy of GMPP estimator technique and also the method proposed doesn't detect shading condition.

In this paper, a novel GMPPT technique is introduced. The technique basis belongs to the artificial vision approach with two main difference, the proposed technique can detect partial shading conditions easily without the need for any extra measurements, secondly, the technique directly estimates the position of the GMPP precisely based on an accurate two-diode model for the PV system. The proposed technique was tested through simulation and practical experimentation, where results show precise shading detecting, accurate irradiance estimation, and accurate estimation for GMPP.

The rest of the paper is structured as follows. Section (2) set the basis for the PV modeling process. Section (3) presents the detection algorithm approach. Section (4) presents the irradiance level calculations based on image processing. In section (5), the experimental setup is conducted to track the global maximum power point using the proposed technique. Section (6) simulation of various shading pattern detection on a single PV module. Finally, the conclusion is drawn based on the obtained results.

2 PV Model

PV module exhibits a non-linear characteristic, to mathematically emulates this behavior various PV modeling techniques are used as the single-diode model, two-diode model, three diode model, multi-diode model, diffusion model, reverse diode model. Among these various approaches, a single diode model is the most used one due to its simplicity yet accuracy. Although the accuracy of the single-diode model drops with low irradiance which makes the two-diode model a better solution with reasonable computations.
The output current for the two-diode model is shown in equation (1)

$$I = I_{PV} - I_{S1} * \left[\exp\left(\frac{q * (V_D + I * R_S)}{a_1 KT}\right) - 1\right] - \frac{V_D + I * R_S}{R_P} - I_{S2} * \left[\exp\left(\frac{q * (V_D + I * R_S)}{a_2 KT}\right) - 1\right] \quad (1)$$

A variety of meta-heuristic techniques are adopted to solve the two-diode model equation to extract the model parameters as particle swarm, genetic algorithm, differential evolution algorithm, firefly algorithm& whale optimization algorithm [11],[12],[13],[14].
In this study, an HFPA-CSA is adopted [15] to extract the seven unknown parameters of the two-diode model based on five test points shown in Table (1) for the Fosera FS1.5 PV module, extracting those parameters help accurately trace the P-V characteristics of the PV module.

Table 1. Five Test Points for FS1.5 PV Module.

Test Point	Current (A)	Voltage (V)
Short-Circuit	0.37	0
Open-Circuit	0	5.33
Maximum PowerPoint	0.34	4.33
Half open-circuit voltage	0.36	2.70
Average of maximum power voltage and open-circuit voltage	0.24	4.91

The objective function used is the absolute error experimental current and model current as shown in equation (2), based on five experimental points for the FS1.5 module.

$$F_{OBJ} = Absolute\ (\ I_{EXP} - I_{Model}\ ) \tag{2}$$

HFPA-CSA was used to minimize the objective function in equation (2), the results give an objective function value of $8.9*10^{-4}$ indicating precise optimization process and the obtained PV Model parameters shown in Table (2).

Table 2. Two-Diode Model Parameters at STC.

Parameter	Value
I_{o1}	5.74e-12 A.
I_{pv}	0.3712 A.
a_1	0.5133.
R_p	300 Ω.
R_s	0.69 Ω.
I_{o2}	6.8102e-12 A
a_2	0.469.

3 Partial Shading Conditions Detection Based on Artificial Vision

3.1 Camera Response function

Digital images are built up from several pixels, where the intensity of these pixels is proportional to the incident light on the captured object. Unfortunately, this relation is a non-linear relation called Camera Response Function (CRF), and it's mainly a camera feature regardless of the surrounding [16]. Various techniques are used to extract the CRF, one of the simplest and effective methods is to capture the same scene at various exposure duration [10]. A Nikon D3400 camera was used to capture the same scene at six different exposure duration, namely: 1/100 Sec, 1/200 Sec, 1/250 Sec, 1/400 Sec, 1/800 Sec, 1/1250 Sec.
Nikon D3400 roughly costs $400 which doesn't affect the project cost, especially for huge power plants, making use of the already available surveillance cameras. Matlab 2019b built-in camera response function was used to obtain the response function of the used camera. The obtained CRF for the Red, Green, and Blue (RGB) components of the image are shown in Figure (1).

The obtained CRF shows the relation between the pixel intensity ranging from (0 to 255) and the incident irradiance, although it is worth pointing out that the irradiance value on the Y-axis is not the absolute incident irradiance but a scaled value of it. Finally, obtaining the CRF is a one-time procedure for a specific camera and doesn't require extensive measurements or installation in the field after that.

3.2 Partial Shading Detection

This section introduces an artificial vision-based algorithm to detect the presence of PS conditions on the PV array. In the previous section, the scaled irradiance of each PV module can be easily computed using the obtained CRF, where the average pixel intensity of each PV module is mapped through the CRF to get the corresponding scaled irradiance incident on each module. Then, if all the modules have the same scaled irradiance level, there is no shading condition, else partial shading condition is detected without extra installation or more computations. The steps for partial shading detection algorithm is shown in Figure (2)

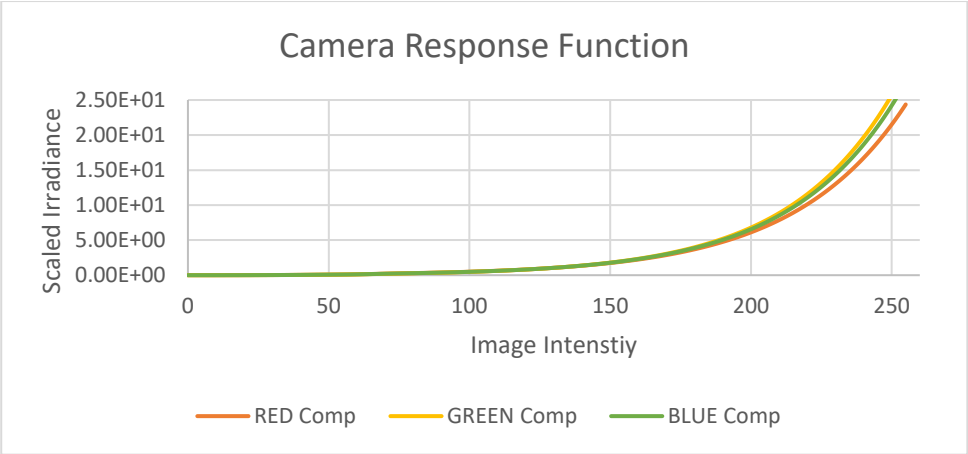

Figure 1. CRF for Nikon D3400 Camera.

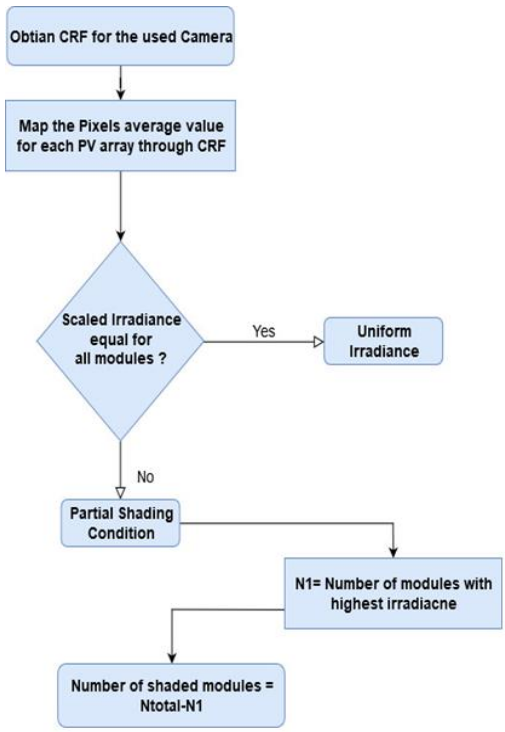

Figure 2. Steps for Partial Shading Detection.

4 Irradiance Calculation Based on Artificial Vision

The previous section detects the presence of the PS condition on the PV array with the number of shaded modules, although the exact irradiance on each module is unknown as the obtained irradiance level is a scaled irradiance.

To get the exact irradiance level, a reference PV module is used with a known incident irradiance. Figure (3) shows an FS1.5 module subjected to 200 w/m^2, with a short-circuited current of 74 mA. The module image was captured with the previously obtained CRF camera to act as a reference module for the scaled irradiance, this captured image will solve the problem of the scaling factor of the camera and the reflection of light on the surface of FS1.5 PV modules.

Table (3) shows the image average scaled irradiance for the RGB components of the captured image.

Having a reference irradiance level of 200 w/m^2 and its corresponding scaled value on the CRF curve, any given scaled irradiance can be calculated.
A simple mathematical calculation can get the real irradiance level for a given scaled irradiance level by simply multiplying the ratio between (given scaled irradiance and the reference scaled irradiance) by 200 as shown in equation (3)

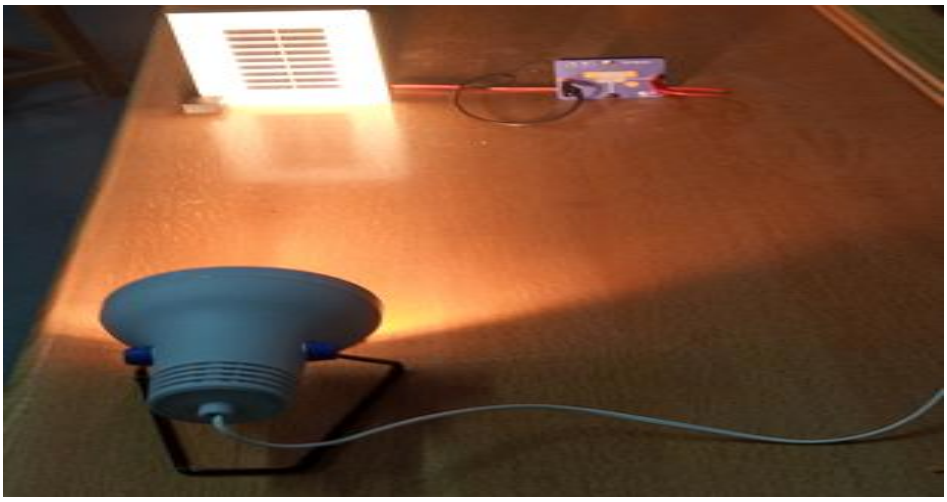

Figure 3. Experimental Setup for FS1.5 module at 200 w/m^2.

$$Irr_{module} = \frac{Scaled\ irradiance_{Module}}{Scaled\ irradiance_{Ref}} * 200 \tag{3}$$

Given that the CRF curve provides three scaled values for the RGB components, equation (3) was modified to take the average scaled value of the RGB component as shown in equation (4)

$$Irr_{module} = \frac{\frac{R_m}{R_{ref}} + \frac{G_m}{G_{ref}} + \frac{B_m}{B_{ref}}}{3} * 200 \tag{4}$$

Where R_m, G_m, B_m are the mapped average values for the RGB components respectively of the captured module image and R_{ref}, G_{ref}, B_{ref} are the mapped average values for the RGB components respectively of the reference module image.

Table 3. Average Mapped values for RGB image.

Average of R-Component	0.0045
Average of G-Component	0.0045
Average of B-Component	0.041

5 Global Maximum PowerPoint Tracking Based on Artificial Vision

To validate the accuracy of the proposed GMPPT algorithm in locating the GMPP using the captured images of the modules and the two-diode model, a PV array consists of three series-connected FS1.5 modules each connected with anti-parallel bypass diode was used as shown in Figure (4). Three light sources were directed to each PV module to have a different irradiance level.

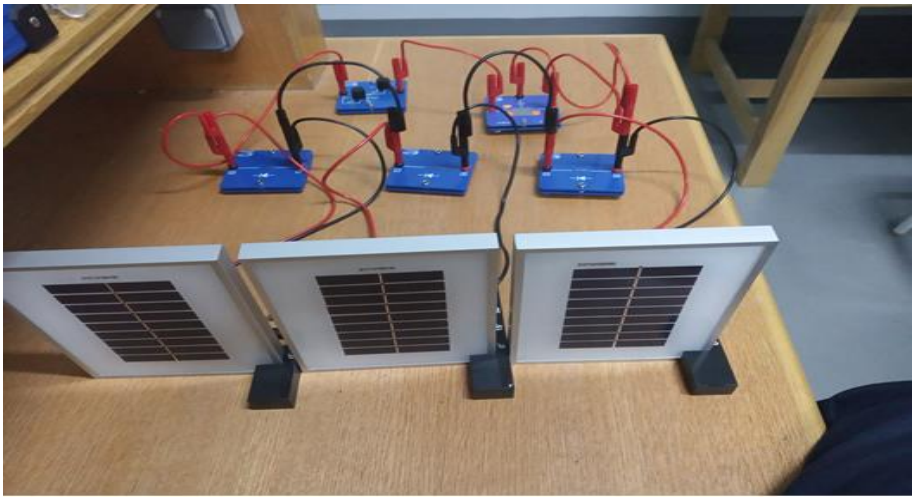

Figure 4. Experimental Setup Partially Shaded PV Array.

The image of each of the three PV modules was captured, the mean of the mapped values for each image was calculated and listed in Table (4)

Table 4. Average Mapped Intensity Values for The Three PV Modules.

Module No.1	
Aver. of R-Component	0.0104
Aver. of G-Component	0.0104
Aver. of B-Component	0.0814
Module No.2	
Aver. of R-Component	0.0077
Aver. of G-Component	0.0077
Aver. of G-Component	0.0711
Module No.3	
Aver. of R-Component	0.0227
Aver. of G-Component	0.0227
Aver. of B-Component	0.2098

Using equation (4) the incident irradiance on each PV module was estimated as follow module No.1 has an incident irradiance level of 1009 w/m^2, module No.2 has an incident irradiance level of 438 w/m^2, module No.3 has an incident irradiance level of 342 w/m2.
The actual incident level on each PV module was measured and found to be 1000 w/m^2, 400 w/m^2, 350 w/m2 respectively, which results in a mean square error (MSE) for the obtained irradiance levels of approximately 23 w/m^2 which is a very satisfying result, especially when referring the irradiance level to the standard irradiance level of 1,000 w/m^2.
The second step after obtaining the irradiance level of each PV module is to obtain the P-V curve for the whole PV array to locate the GMPP.

The Simulink model was constructed compromising three series-connected FS1.5 PV modules using the previously obtained two-diode parameters to plot the P-V curve knowing the irradiance level of each module to be 1009, 438, and 342 w/m^2 respectively. The obtained P-V and I-V curves are shown in figure (5).
The obtained simulated points on the previous curves for the power, voltage, and current were stored in a memory slot. The P-V curve is scanned using the Matlab built-in maximum function to locate the GMPP and the corresponding voltage and current.

The GMPP was found to be at a voltage of 14 V and 0.12 A giving a global maximum power of 1.7 w. The steps for GMPPT algorithm are shown in Figure (6). Experimental points were measured along the I-V and P-V curves to locate the GMPP practically where the GMPP was found to be located at a voltage of 14V and 0.12 A with 1.7 w of extracted power.

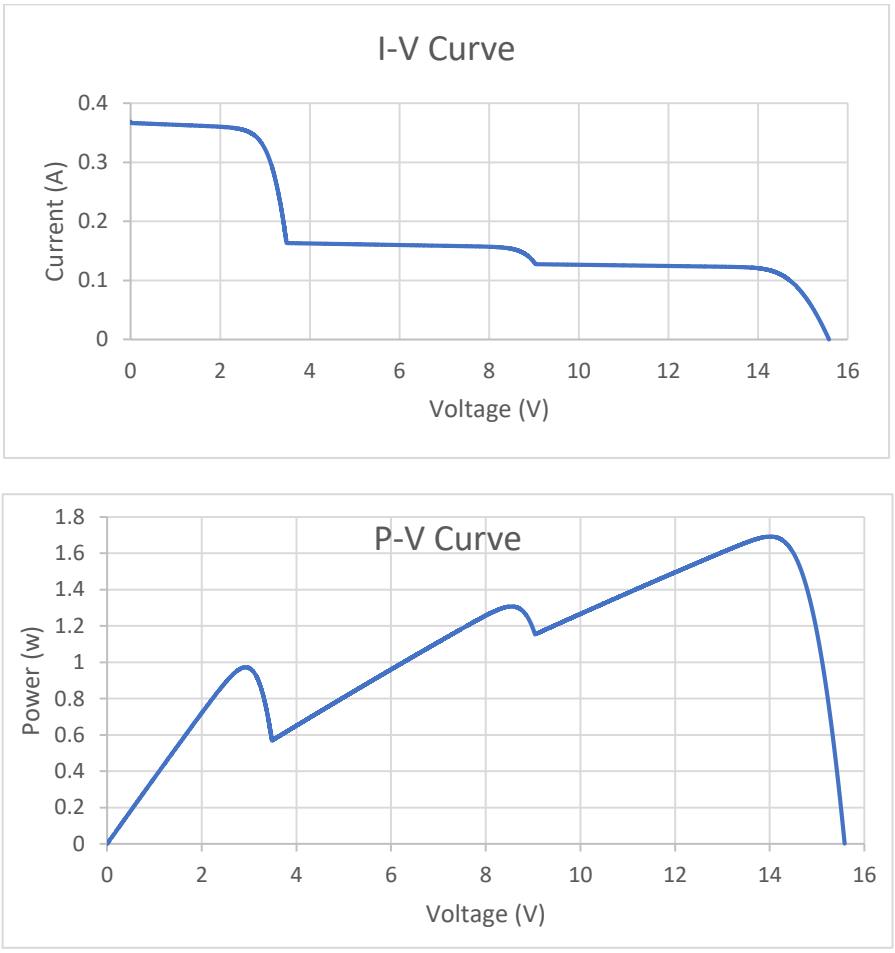

Figure 5. Simulated I-V & P-V Curves for the Shaded PV Array.

It can be seen that the simulated model located the GMPP precisely. To ensure the validity of results, another shading scenario was explored with two series-connected PV modules where the estimated irradiance levels were found to be of 1009 and 438 w/m^2 respectively. The simulated model locates the GMPP at a voltage of 9.3 V and 0.15 A giving a global maximum power of 1.4 w, experimental measurement locate the GMPP at a voltage of 9.3 V and 0.14 A giving a global maximum power of 1.37 w. Again, the simulated model precisely locates the GMPP with only an error of 0.01 in the current and power measurement.

6 Detecting Shaded Cells on a PV Module

So far, the proposed algorithm estimates the incident irradiance level on a given PV module by referring its average mapped pixel intensity to the reference module. This hypothesis stays true if the shaded module suffers a uniform irradiance on its surface, while if the PV module itself is partially shaded having part of its area shaded and the rest faces the normal irradiance level the estimated irradiance is wrong.

To solve this issue the region suffering a shadow in the PV module should be detected thus splitting the PV module into two regions, where each region irradiance level is estimated separately. This shadow detection approach helps to correctly estimate the incident irradiance level on the PV Module correctly, furthermore, detect the shaded parts in a PV module helps to predict hotspots formation and limit it if possible.

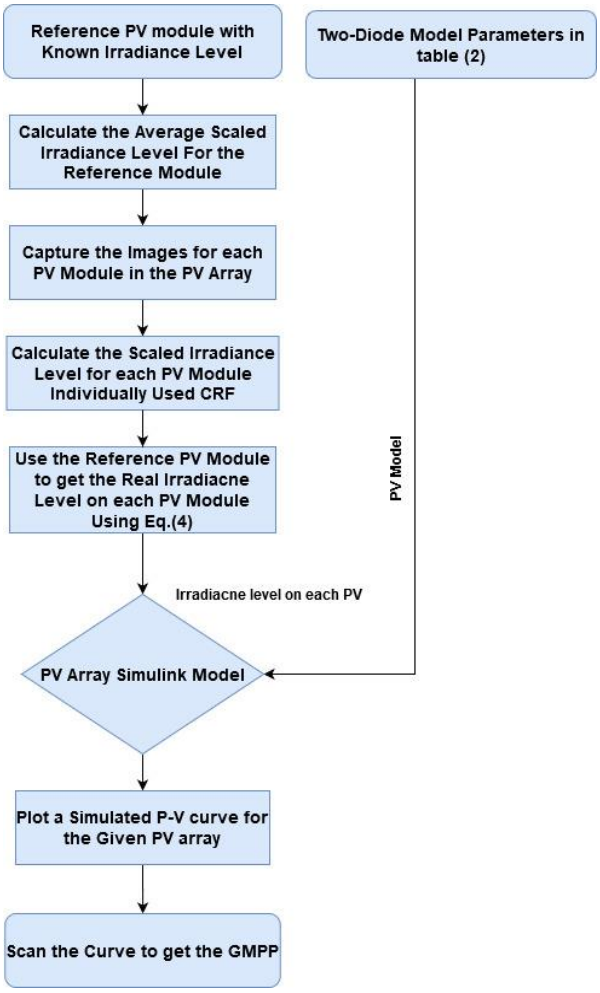

Figure 6. Steps for GMPPT.

The algorithm for shadow detection for a given PV module is as follows. The RGB image captured is converted to Hue Saturation Value (HSV) color space, HSV color space is chosen due to its ability to separate both pixel intensity and chroma components [17]. The obtained HSV image is thresholded to separate the shadow region.

The obtained thresholded image is manipulated by the morphological opening operation to remove any unwanted details in the obtained image [18], finally, the shadow boundary is detected. Shadow detection algorithm was tested against a shading pattern on a single PV module as shown in Figure (7).

Firstly, the module picture is captured in RGB color space as shown in Figure 7(a), then the captured image is converted to HSV color space to distinguish the shadow area which is shown as a green area in figure 7(b), thresholding process isolates the shadow area from the rest of module area to form a binary image compromising the shadow area in white color and the rest of the module in black color, extra details or voids in the image is excluded using the opening operation to produce the binary image shown in Figure 7(c), finally, Figure 7(d) shows a frame plotted around the shadow area presenting the number of shaded cells in the PV module. Matlab 2019a built-in image processing toolbox was utilized to convert the RGB to HSV color space and perform the thresholding process.

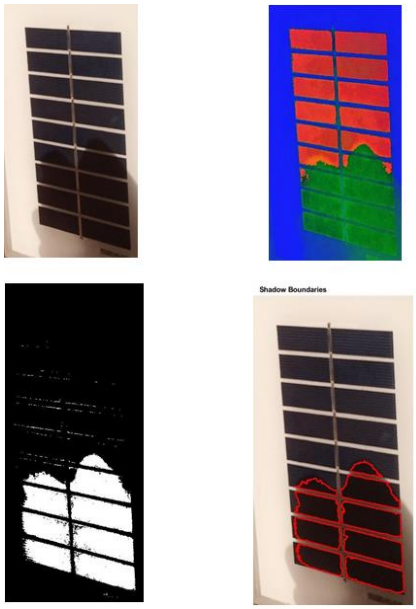

Figure 7. Detecting Shadow pattern (3) on a PV module.

a) RGB Image b) HSV image c) Threshold Binary Image d) Shadow detected area

It can be seen that the shadow area was correctly detected for each given shadow pattern. Where there are nine shaded cells "outlined with the red line".

7 Conclusions

This paper presents an accurate partial shading detection algorithm and a GMPPT algorithm based on the captured images of the PV array.
The only used piece of equipment was the Nikon D3400 camera.
The first step was to estimate the CRF for the used camera as shown in Figure 1.
The obtained CRF was used to detect the presence of partial shading conditions on the PV panels with a simple, cheap, and accurate technique as shown in Figure 2.
The second step involves estimating the real irradiance level on each PV panel which was estimated with the aid of a reference PV at 200 w/m^2.
To detect the GMPP the estimated irradiance level for each PV panel was fed to a Simulink model of the given PV array using the two-diode model parameters' obtained at table (2).
The Simulink model was used to plot the simulated P-V characteristics for the whole PV array and scan the obtained curve to get the simulated GMPP.
Finally, the obtained simulated GMPP was compared with the practical GMPP showing an excellent detection behavior for the proposed GMPPT algorithm.
The steps of the GMPPT is shown in Figure (5).
Another modification for the proposed GMPPT algorithm in section (6) to detect the shaded cells in case the PV panel itself suffers a partial shading in its cells.

The proposed algorithm successfully detects partial shading conditions across PV panels and PV cells, track the GMPP with high accuracy regardless of the shading scenario. The proposed algorithm depends on simple artificial vision operations. There is no expensive equipment needed only a normal camera is required whose price is incomparable to the system cost, neither a sophisticated controller is needed nor a complicated artificial intelligence is required.
The image processing tools used are all available in the Matlab 2019b version.

The proposed algorithm was tested against a PV array consisting of three series PV modules, although the technique can be used for larger PV arrays as its accuracy in independent to system configuration, the system accuracy mainly depends on the accuracy of the obtained CRF and the two-diode model parameters.

Further improvement for these two factors will improve the proposed technique accuracy when dealing with large a PV array.

References

[1] W. Kreft, M. Filipowicz, and M. Żołądek, "Reduction of electrical power loss in a photovoltaic chain in conditions of partial shading," *Optik*, vol. 202, no. October 2019, p. 163559, 2019.

[2] J. C. Teo, R. H. G. Tan, V. H. Mok, V. K. Ramachandaramurthy, and C. Tan, "Impact of bypass diode forward voltage on maximum power of a photovoltaic system under partial shading conditions," *Energy*, vol. 191, p. 116491, 2019.

[3] B. Yang *et al.*, "Comprehensive overview of maximum power point tracking algorithms of PV systems under partial shading condition," *Journal of Cleaner Production*, vol. 268, p. 121983, 2020.

[4] S. M. Hashemzadeh, "A new model-based technique for fast and accurate tracking of global maximum power point in photovoltaic arrays under partial shading conditions," *Renewable Energy*, vol. 139, pp. 1061–1076, 2019.

[5] S. M. Hashemzadeh and M. Hejri, "A Fast and Accurate Global Maximum Power Point Tracking Method for Solar Strings Under Partial Shading Conditions," *Journal of Operation and Automation in Power Engineering*, 2020.

[6] D. Yousri, D. Allam, and M. B. Eteiba, "Optimal photovoltaic array reconfiguration for alleviating the partial shading influence based on a modified harris hawks optimizer," *Energy Conversion and Management*, vol. 206, no. December 2019, p. 112470, 2020.

[7] A. K. Ryad, A. M. Atallah, and A. Zekry, "Photovoltaic array reconfiguration under partial shading based on integer link matrix and harmony search," *European Journal of Electrical Engineering*, vol. 21, no. 5, pp. 471–477, 2019.

[8] P. R. Satpathy and R. Sharma, "Power recovery and equalization in partially shaded photovoltaic strings by an efficient switched capacitor converter," *Energy Conversion and Management*, vol. 203, no. September 2019, p. 112258, 2019.

[9] A. D. Martin, J. R. Vazquez, and J. M. Cano, "MPPT in PV systems under partial shading conditions using artificial vision," *Electric Power Systems Research*, vol. 162, no. April, pp. 89–98, 2018.

[10] Y. Mahmoud and E. F. El-Saadany, "A Novel MPPT Technique Based on an Image of PV Modules," *IEEE Transactions on Energy Conversion*, vol. 32, no. 1, pp. 213–221, 2017.

[11] D. S. Pillai and N. Rajasekar, "Metaheuristic algorithms for PV parameter identification: A comprehensive review with an application to threshold setting for fault detection in PV systems," *Renewable and Sustainable Energy Reviews*, vol. 82, no. January 2017, pp. 3503–3525, 2018.

[12] A. M. Humada, M. Hojabri, S. Mekhilef, and H. M. Hamada, "Solar cell parameters extraction based on single and double-diode models : A review," vol. 56, pp. 494–509, 2016.

[13] A. Mohammad and A. Maroosi, "Parameter identi fi cation for solar cells and module using a Hybrid Fire fly and Pattern Search Algorithms," *Solar Energy*, vol. 171, no. November 2017, pp. 435–446, 2018.

[14] G. Xiong, J. Zhang, D. Shi, and Y. He, "Parameter extraction of solar photovoltaic models using an improved whale optimization algorithm," vol. 174, no. March, pp. 388–405, 2018.

[15] A. K. Ryad, A. M. Atallah, and A. Zekry, "Photovoltaic Parameters Estimation Using Hybrid Flower Pollination with Clonal Selection Algorithm," *Turkish Journal of Electromechanics and Energy*, vol. 3, no. 2, pp. 15–21, 2018.

[16] C. Chen, S. McCloskey, and J. Yu, "Image splicing detection via camera response function analysis," in *30th IEEE Conference on Computer Vision and Pattern Recognition, CVPR 2017*, 2017, vol. 2017-Janua, pp. 1876–1885.

[17] B. Hdioud, M. E. H. Tirari, R. O. H. Thami, and R. Faizi, "Detecting and shadows in the HSV color space using dynamic thresholds," *International Journal of Electrical and Computer Engineering*, vol. 8, no. 3, pp. 1513–1521, 2018.

[18] Z. H. Roslan, J. H. Kim, R. Ismail, and R. Hamzah, *Tree crown detection and delineation using digital image processing*, vol. 935. 2019.